Template-Directed Self-Assembly of Alkanethiol Monolayers: Selective Growth on Preexisting Monolayer Edges

Ruben B. A. Sharpe,[†] Dirk Burdinski,*[,‡,§] Jurriaan Huskens,*[,†,⊥,#] Harold J. W. Zandvliet,*[,†,▽] David N. Reinhoudt,[†,#] and Bene Poelsema[†,▽]

MESA+ Institute for Nanotechnology and Faculty of Science and Technology, University of Twente, P.O. Box 217, 7500 AE Enschede, The Netherlands, and Philips Research, High Tech Campus Eindhoven, 5656 AE Eindhoven, The Netherlands

Received June 21, 2006. In Final Form: October 12, 2006

Self-assembled monolayers were investigated for their suitability as two-dimensional scaffolds for the selective growth of alkanethiol edge structures. Heterostructures with chemical contrast could be grown, whose dimensions were governed by both the initial pattern sizes and the process time. *n*-Octadecanethiol (ODT) was made to expand from the edges of 16-mercaptohexadecanoic acid (MHDA) monolayer patterns. Likewise, 11-mercaptoundecanol (MUD) was grown on MHDA and on ODT monolayer edges. The results of these experiments are in accordance with the moving boundary model for monolayer spreading. In addition to such surface-bound spreading, a vapor-phase contribution to lateral monolayer growth was identified. MUD was observed to be an excellent ink for creating chemical contrast by means of regioselective deposition from a vapor phase. As a proof of principle, ribbons of 11-mercaptoundecanol with submicrometer widths were grown on pentaerythritol-tetrakis(3-mercaptopropionate) edges, and submicrometer wide gold lines were produced by subsequent wet-chemical etching.

Introduction

The incessant demand for miniaturization in electronics, medical, and nanotechnology is currently met by the development of fabrication methods of ever-increasing complexity and cost. Soft-lithographic patterning techniques offer the potential for an alternative low-cost, large-area, and high-volume production technology.[1,2] Microcontact printing (μCP) is a particularly easy and versatile representative of the soft lithography family and has received a lot of attention in recent years.[2−4] In μCP self-assembled monolayers (SAMs) of amphiphilic nature, usually organic molecules are formed on the surface of a substrate only in the areas of contact with the ink-loaded soft lithography mask (stamp). With decreasing feature size, the mechanical stability of the utilized stamps becomes a limiting factor.[2,5−12] This challenge has to be met by materials that are by definition soft and flexible.

An interesting novel approach to circumvent this problem is the creation of submicrometer patterns by using masks with micrometer-sized features, which are characterized by a higher mechanical stability and are therefore easier to produce and handle. Edge lithographic techniques utilize the edges of such large pattern features to determine submicrometer-sized structures. Examples include near-field phase-shifting photolithography,[13,14] topographically directed etching,[15,16] edge transfer lithography,[17] and controlled undercutting.[18]

Because of their inherent mobility, the use of self-assembled alkanethiol monolayers in edge lithographic schemes would, in principle, allow for control of edge-feature sizes by controlling the process time. Edge-spreading lithography (ESL), an edge lithographic technique that exploits the propensity of alkanethiol SAMs for spreading, has recently been reported.[19,20] In this technique, the ink source (an inked rubber stamp) is decoupled from the substrate by freestanding structures on the substrate that act as physical guides for the spreading process. It is a multistep technique that requires the compatibility of the techniques for creating the guiding structures with that of the

* To whom correspondence should be addressed. dirk.burdinski@philips.com (D.B.); j.huskens@utwente.nl (J.H.); h.j.w.zandvliet@utwente.nl (H.J.W.Z.).

[†] University of Twente.

[‡] High Tech Campus Eindhoven.

[§] Bio-Molecular Engineering, Philips Research.

[⊥] MESA+ Strategic Research Orientation "Nanofabrication".

[#] Supramolecular Chemistry and Technology, University of Twente.

[▽] Solid State Physics, University of Twente.

(1) Xia, Y.; Whitesides, G. M. *Angew. Chem., Int. Ed.* **1998**, *37*, 550−575.

(2) Michel, B.; Bernard, A.; Bietsch, A.; Delamarche, E.; Geissler, M.; Juncker, D.; Kind, H.; Renault, J.-P.; Rothuizen, H.; Schmid, H.; Schmidt-Winkel, P.; Stutz, R.; Wolf, H. *IBM J. Res. Dev.* **2001**, *45*, 697−719.

(3) Kumar, A.; Whitesides, G. M. *Appl. Phys. Lett.* **1993**, *63*, 2002−2004.

(4) Delamarche, E.; Schmid, H.; Bietsch, A.; Larsen, N. B.; Rothuizen, H.; Michel, B.; Biebuyck, H. *J. Phys. Chem. B* **1998**, *102*, 3324−3334.

(5) Hui, C. Y.; Jagota, A.; Lin, Y. Y.; Kramer, E. J. *Langmuir* **2002**, *18*, 1394−1407.

(6) Schmid, H.; Michel, B. *Macromolecules* **2000**, *33*, 3042−3049.

(7) Bietsch, A.; Michel, B. *J. Appl. Phys.* **2000**, *88*, 4310−4318.

(8) (a) Sharp, K. G.; Blackman, G. S.; Glassmaker, N. J.; Jagota, A; Hui, C.-Y. *Langmuir* **2004**, *20*, 6430−6438. (b) Decré, M. J. J.; Timmermans, P. H. M.; van der Sluis, O.; Schroeders, R. *Langmuir* **2005**, *21*, 7971−7978.

(9) (a) Trimbach, D.; Feldman, K.; Spencer, N. D.; Broer, D. J.; Bastiaansen, C. W. M. *Langmuir* **2003**, *19*, 10957−10961. (b) Tormen, M.; Borzenko, T.; Steffen, B.; Schmidt, G.; Molenkamp, L. W. *Microelectron. Eng.* **2002**, *61*−*62*, 469−473. (c) Odom, T. W.; Love, J. C.; Wolfe, D. B.; Paul, K. E.; Whitesides, G. M. *Langmuir* **2002**, *18*, 5314−5320.

(10) Li, H.-W.; Muir, B. V. O.; Fichet, G.; Huck, W. T. S. *Langmuir* **2003**, *19*, 1963−1965.

(11) Decré M. M. J.; Schneider, R.; Burdinski, D.; Schellekens, J.; Saalmink, M.; Dona, R. *Mater. Res. Soc. Symp. Proc.* **2004**, *EXS-2*, 59−61.

(12) Delamarche, E.; Vichiconti, J.; Hall, S. A.; Geissler, M.; Graham, W.; Michel, B.; Nunes, R. *Langmuir* **2003**, *19*, 6567−6569.

(13) Rogers, J. A.; Paul, K. E.; Jackman, R. J.; Whitesides, G. M. *Appl. Phys. Lett.* **1997**, *70*, 2658−2660.

(14) Rogers, J. A.; Paul, K. E.; Jackman, R. J.; Whitesides, G. M. *J. Vac. Sci. Technol. B* **1998**, *16*, 59−68.

(15) Aizenberg, J.; Black, A. J.; Whitesides, G. M. *Nature* **1998**, *394*, 868−871.

(16) Black, A. J.; Paul, K. E.; Aizenberg, J.; Whitesides, G. M. *J. Am. Chem. Soc.* **1999**, *121*, 8356−8365.

(17) (a) Cherniavskaya, O.; Adzic, A.; Knutson, C.; Gross, B. J.; Zang, L.; Liu, R.; Adams, D. M. *Langmuir* **2002**, *18*, 7029−7034. (b) Sharpe, R. B. A.; Titulaer, B. J. F.; Peeters, E.; Burdinski, D.; Huskens, J.; Zandvliet, H. J. W.; Reinhoudt, D. N.; Poelsema, B. *Nano Lett.* **2006**, *6*, 1235−1239.

(18) Love, J. C.; Paul, K. E.; Whitesides, G. M. *Adv. Mater.* **2001**, *13*, 604−607.

(19) McLellan, J. M.; Geissler, M.; Xia, Y. *J. Am. Chem. Soc.* **2004**, *126*, 10830−10831.

(20) Geissler, M.; McLellan, J. M.; Xia, Y. *Nano Lett.* **2005**, *5*, 31−36.

10.1021/la061787v CCC: $37.00
Published on Web 12/08/2006

actual edge-spreading. A more convenient approach would be the use of a SAM itself to act as the physical guide. Compatibility is then inherent. Such a scheme has recently been reported in a study of molecular transport across existing monolayers using dip-pen nanolithography (DPN).[21,22]

Apart from the technological advantages, the use of multiple-ink systems in the DPN study led to a better understanding of the role of the liquid meniscus in the spreading mechanism of DPN. Likewise, the use of multiple-ink systems may yield new insight in the process of monolayer spreading in μCP. From the literature, it is suggested that the spreading of monolayer patterns occurs by means of excess molecules that migrate across the completed dense monolayer areas, being incorporated in the SAM at its edges.[4,23−29] The monolayer-covered regions and the bare substrate thus constitute domains that have different properties with respect to thiol transport. The boundary between those domains continually shifts as a result of the transport itself. Models for such "moving boundary transport" have been adapted from heat conduction theory to the process of spreading in DPN.[29−33] There are, however, several relevant differences between DPN and μCP. Most significantly, in contrast to μCP, in DPN there is no contribution from within the ink transfer medium (the tip material), there is a limited solvent presence, and the transport takes place in ambient conditions, as opposed to within the confinements of a microcavity enclosed by the stamp material and substrate. These complicating contributions have to be considered in a description of the spreading behavior of ink molecules across the preformed part of a monolayer in μCP.

In this report, the feasibility is shown of an ESL scheme, in which a microcontact printed monolayer serves as the physical guide. Moreover, it is shown that, because of the properties of the stamp environment, selective edge growth can be accomplished, even if there is no direct contact between the ink source and the preexisting monolayer pattern. This entails area-selective deposition from a vapor phase and calls for a refinement of the model for spreading in μCP.

Experimental Section

Materials and Methods. Gold substrates (20 nm of evaporated gold on a 5-nm adhesion layer of evaporated titanium, on top of an ∼250-nm thermal silicon oxide) were prepatterned using μCP. The stamp material, Sylgard-184 poly(dimethylsiloxane) (PDMS), was obtained from Dow Corning. It was mixed in a 1:10 curing agent/prepolymer ratio and cured overnight at 60 °C. The PDMS stamps were used without further treatment.

16-Mercaptohexadecanoic acid (MHDA, 90% purity), *n*-octadecanethiol (ODT, 98% purity), 11-mercaptoundecanol (MUD, 97% purity), and pentaerythritol-tetrakis(3-mercaptopropionate) (PTMP, 96% purity) were purchased from Sigma-Aldrich. All materials were used as received. Ink solutions were prepared by dissolution of the appropriate compounds in ethanol. Solutions of 2 mM ODT (only for the prepatterning steps), 10 mM ODT (for all growth experiments), 10 mM MHDA and 10 mM MUD (for both the prepatterning steps and the growth experiments), and 1 mM PTMP in ethanol were used.

Stamps were inked by submersion in the corresponding ink solution for at least 1 h. Prior to use, the substrates were successively rinsed with ultrapure water (resistivity > 18.2 MΩ cm), ethanol, and heptane and dried in a stream of nitrogen. Ethanol and heptane (both p.a. grade) were purchased from Merck. The gold substrates were thereafter exposed to a Tepla 300E microwave argon plasma (300 W, 0.25 mbar Ar) for 5 min immediately preceding printing.

The substrates were prepatterned with the appropriate template monolayers by means of μCP for 15 s. Lateral growth of these patterns was effected either by direct contact of an inked stamp with the prepatterned substrate areas, or by the uniform application of a vapor of a suitable ink. The vapor spontaneously emerged within the confinements of the recessed areas of an inked stamp and the substrate during a second printing step. The first and second printing steps were made with stamps bearing identical patterns. The stamp orientation during the second printing step was rotated by approximately 45° with respect to the pattern on the substrate, so that partial overlap of the structures occurred. The amount of ink that was transferred in this second step was varied by variation of the contact time between the inked stamp and the gold. Contact times were varied from 15−300 s. Because of significant variations in the degree of time-dependent spreading, the *extent* of spreading, instead of the *contact time*, is reported.

Characterization. The samples were etched using a standard thiosulfate-based etch bath, to which octanol was added at half saturation, in order to decrease the sensitivity for pin-holes.[34,35] Optical micrographs were obtained from etched substrates. Additionally, atomic force microscopy (AFM) images were taken of non-etched patterns. For AFM characterization, a Veeco MultiMode scanning probe microscope was used in conjunction with a Nanoscope IIIa controller. The AFM was operated in contact mode (cm-AFM), and chemical contrast was gauged from the observed contrast in friction force (ff-AFM).

Software for Analysis. Images were analyzed using ImageJ, a public domain image processing program by the U.S. National Institutes of Health (NIH),[36] and Nanotec's WSxM, a freeware data acquisition and processing program for scanning probe microscopy.[37]

Results

ODT on MHDA and Vice Versa. Conceptually, the process of monolayer spreading in μCP may be mimicked by a two-step process, in which first a template monolayer is formed and subsequently an ink source is applied on top of this preformed monolayer (Figure 1). In order to obtain contrast, ODT ink was applied on a preformed MHDA pattern and vice versa. ODT-covered surface areas can be distinguished from bare gold surfaces based on a lower signal intensity in ff-AFM images, whereas MHDA coverage results in areas of higher intensity (Figure 2). The pattern of interest on the stamp comprised for both inks of an array of 10×10 μm^2 squares that were spaced 10 μm apart. A first monolayer pattern was created in a printing step of 15 s, which, for both inks, did not cause a noticeable increase in feature size. The second ink was applied in a second printing step of t s ($30 < t < 300$). The size increase of the features in this second printing step is a measure of the maximum amount

(21) Piner, R. D.; Zhu, J.; Xu, F.; Hong, S.; Mirkin, C. A. *Science* **1999**, *283*, 661−663.
(22) Hampton, J. R.; Dameron, A. A.; Weiss, P. S. *J. Am. Chem. Soc.* **2006**, *128*, 1648−1653.
(23) Ulman, A. *Chem. Rev.* **1996**, *96*, 1533−1554.
(24) Schreiber, F. *Prog. Surf. Sci.* **2000**, *65*, 151−256.
(25) Poirier, G. E.; Pylant, E. D. *Science* **1996**, *272*, 1145−1148.
(26) Poirier, G. E. *Langmuir* **1997**, *13*, 2019−2026.
(27) Poirier, G. E.; Fitts, W. P.; White, J. M. *Langmuir* **2001**, *17*, 1176−1183.
(28) Sharpe, R. B. A.; Burdinski, D.; Huskens, J.; Zandvliet, H. J. W.; Reinhoudt, D. N.; Poelsema, B. *Langmuir* **2004**, *20*, 8646−8651.
(29) Jang, J.; Hong, S.; Schatz, G. C.; Ratner, M. A. *J. Chem. Phys.* **2001**, *115*, 2721−2729.
(30) Crank, J.; Park, G. S. *Diffusion in Polymers*; Academic Press: New York, 1968; pp 25−27.
(31) Crank, J. *The Mathematics of Diffusion*, 2nd ed.; Clarendon Press: Oxford, 1994; pp 290−297.
(32) Carslaw, H. S.; Jaeger, J. C. *Conduction of Heat in Solids*; Clarendon Press: Oxford, 1959; pp 282−296.
(33) Sheehan, P. E.; Whitman, L. J. *Phys. Rev. Lett.* **2002**, *88*, 156104(4).
(34) Kumar, A.; Biebuyck, H. A.; Whitesides, G. M. *Langmuir* **1994**, *10*, 1498−1511.
(35) Geissler, M.; Schmid, H.; Bietsch, A.; Michel, B.; Delamarche, E. *Langmuir* **2002**, *18*, 2374−2377.
(36) ImageJ Image Processing Program. http://rsb.info.nih.gov/ij/ (accessed Jan 2004).
(37) Nanotec Electronica Homepage. http://www.nanotec.es/ (accessed Jan 2004).

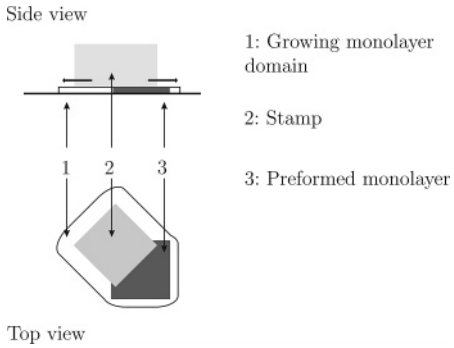

Figure 1. Schematic representation of a suitable stamp/monolayer configuration for monolayer spreading across a preformed monolayer of different composition.

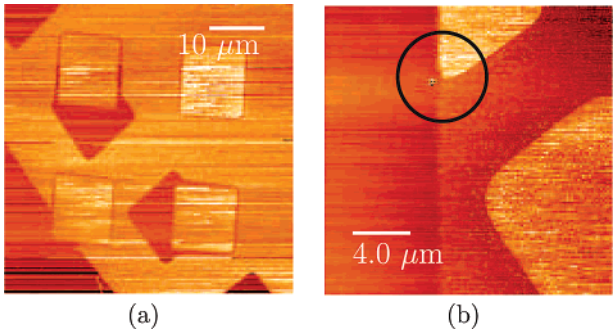

Figure 2. ff-AFM images of preformed MHDA monolayer structures contacted with ODT-inked stamps (a), and of preformed ODT structures contacted with MHDA-inked stamps (b). The contact times were 15 s for the preformed structures and 30 and 300 s for the ODT (a) and MHDA (b) second print, respectively. The picture frames are aligned with the square features of the initial SAM pattern. The dark areas correspond to low lateral interaction, and thus to the ODT monolayers, the bright squares conversely correspond to MHDA monolayers. The area of intermediate intensity, which constitutes the background, corresponds to bare gold. Encircled in panel b is the region where the three domains meet. No such three-domain region is observed for the cases where ODT was printed on top of MHDA patterns.

of feature growth that can be expected from spreading across the template monolayers. The contact time to apply the second pattern was chosen to be sufficiently long to allow for spreading. In the case of printing a layer of ODT on MHDA, after a contact time of 30 s, the feature size of the ODT patterns increased on average to $10.3 \times 10.3\ \mu m^2$ (Figure 2a). In the case of printing a layer of MHDA on ODT, after a contact time of 300 s, the feature size of the MHDA patterns increased on average to $12.0 \times 12.0\ \mu m^2$ (Figure 2b).

A rim of lower intensity was observed to have formed around preformed MHDA features after printing of ODT (Figure 2a), but no evidence was observed for MHDA migration across a preformed ODT pattern (Figure 2b), in spite of the much greater extent of MHDA spreading. It is interesting to note that MHDA spreading alongside an ODT domain resulted in a clearly distinguishable curvature where the three domains (ODT, MHDA, and bare gold) meet (Figure 2b).

When ODT was printed on preformed MHDA patterns, the AFM images revealed a dark rim (indicating ODT presence) around the MHDA features that were not contacted in the ODT printing step (Figures 2a and 3). This is indicative of ODT accumulation at the edges of the MHDA pattern, either by migration across the surface or from the vapor phase.

Because AFM typically probes only a small area of the substrate, another means of characterization was employed to

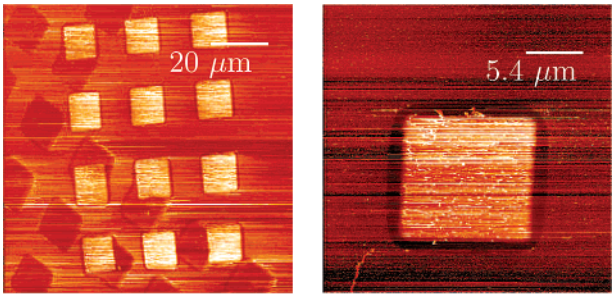

Figure 3. ff-AFM images of a preformed MHDA pattern (high-intensity patches) that was subjected to a subsequent ODT printing step. The dark patches correspond to regions of lower friction and are associated with ODT monolayers. Dark regions were even found to circumscribe bright patches, although they had not been in direct contact with the ODT-inked stamp.

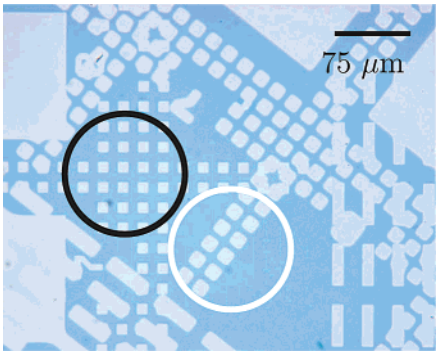

Figure 4. Optical micrograph of ODT monolayer features grown on a preformed MHDA monolayer and then etched into a gold-on-silicon substrate. Encircled in black is the pattern of the MHDA SAM that has been extended by the incorporation of ODT. Encircled in white is the pattern of the ODT SAM. Initially, the nominal size of the stamped features in both encircled regions was $10 \times 10\ \mu m^2$, with a 10 μm spacing in the two high-symmetry directions.

quickly gather information on a significantly larger length scale. To this end, the patterns were transferred into the gold substrate by wet chemical etching. The patterns were subsequently evaluated over larger areas by optical microscopy (Figure 4). Because both inks are equally etch resistant under the conditions used, no contrast in functionality between the two different SAMs can be observed with this method. Useful information can nevertheless be derived from comparison of the pattern sizes in three regions on the same sample: (1) The original pattern size as measured from features in the regions that were not exposed to the vapor, that is, in the region that had not been covered during a second printing step; (2) the pattern size of isolated features of the original pattern that were exposed to vapor (Figure 4, encircled in black); (3) the pattern size of isolated features in the region in which, during the second printing step, the stamp made contact with the bare substrate (Figure 4, encircled in white). From comparison of regions 1 and 2, the extent of growth resulting from vapor exposure can be derived. Furthermore, when the features on the stamps are identical for the two printing steps, a comparison of regions 1 and 3 yields the amount of self-spreading during the second printing step. Note that the rate of ODT self-spreading is larger than the rate of extension of the MHDA pattern as a result of ODT-vapor exposure (Figure 4).

The composition of the gas phase is very sensitive to temperature and pressure variations, as is the rate of self-spreading. Because the PDMS stamp is very flexible and thin, the amount of deposition is very hard to control accurately by manually

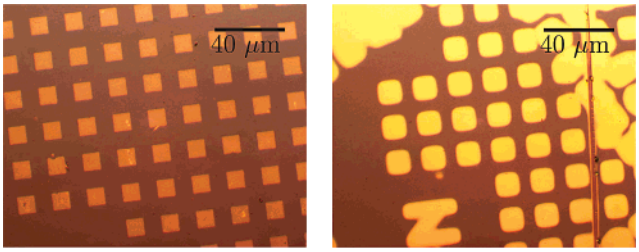

Figure 5. Optical micrographs of etched substrates prepatterned with MUD only (a), and with MUD grown on the preformed MUD pattern on exposed regions of the same sample (b). Growth was effected by vapor-phase exposure of approximately 3 min. A standard etch solution and an etch time of 10 min was used for both samples.[34]

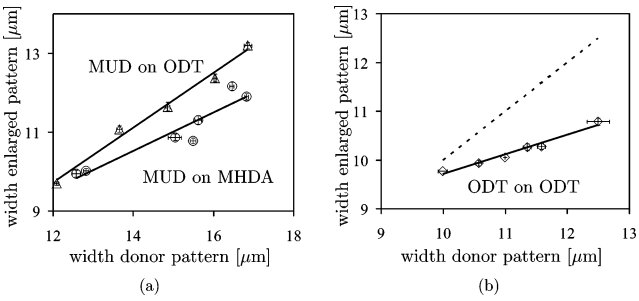

Figure 6. Graphical representation of the extent of feature growth of initially 10 μm features, which comprise a first ink, as a function of the pattern size of the second ink in isolated regions (donor pattern). Panel a shows the results for MUD on ODT (triangles) and for MUD on MHDA (circles). Panel b shows the result for ODT on ODT (diamonds). The dashed line in panel b represents a situation in which the sizes of the donor and the enlarged patterns are equal. The error bars indicate the standard deviation in feature size on *one* substrate, whereas the scatter around the trend line is a measure for the reproducibility between *different* substrates. The drawn lines are guides for the eye.

controlling the contact time. Therefore, the growth of the feature sizes of the second ink is taken as an alternative measure for the vapor exposure.

MUD on MHDA and ODT. MUD was identified as a suitable compound for a scheme to effect monolayer growth from a vapor phase, as is illustrated in Figure 5. Whereas the pattern of the preformed MUD monolayer provided only low etch resistance, it closely followed the contact areas (Figure 5a). Upon exposure to MUD vapor, however, the etch resistance increased significantly while the pattern sizes increased markedly, clearly demonstrating area discrimination during gas-phase deposition (Figure 5b).

In order to assess the rate of edge growth as a function of monolayer composition, which could provide information on the edge growth mechanism, monolayers of MUD were grown on patterns of ODT and MHDA. Comparison of MUD growth on MHDA and ODT shows a clear difference in growth rate (Figure 6a). For the same amount of spreading of the second printed pattern ("donor pattern"), which is taken to be a measure of the interaction between the vapor phase and the substrate, there is a consistent difference in the extent of feature size increase for growth on MHDA and on ODT edges. This indicates that the selective growth is governed by vapor/monolayer interactions. Also, it was found that the monolayer patterns of ODT included at the edges of an ODT template pattern (Figure 6b) were consistently smaller than the corresponding donor pattern.

ODT and MUD on PTMP. The contrast in chemical functionality between the preformed and the subsequently grown

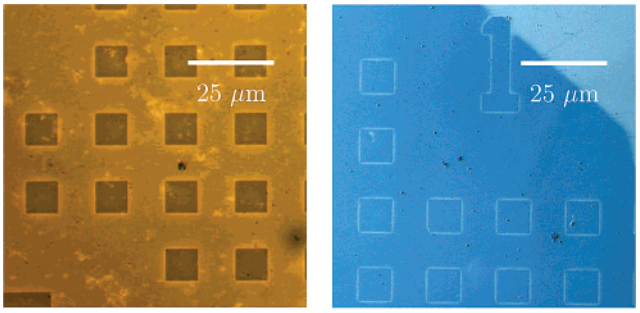

Figure 7. Optical micrographs of etched gold substrates, initially patterned by μCP of PTMP followed by deposition of ODT (a) or MUD (b) in a second printing step. The feature width in image b is 720 $\pm$ 60 nm.

monolayers can be utilized in several ways. As an example, it will be shown in the following that a convenient selection of a monolayer system allows one to accomplish selective transfer of edge structures into a metallic substrate. Delamarche et al. showed that alkanethiol monolayers can be used in conjunction with PTMP to generate etch contrast.[38] The low etch resistance of PTMP SAMs results in preferential etching of the PTMP-covered areas over those that bear alkanethiol SAMs. Figure 7a shows the results of an etch experiment, in which ODT was deposited in a second printing step on a preformed PTMP pattern. Clearly, there was not much contrast in etch resistance between the ODT that was preferentially grown on the PTMP edges and the ODT that was randomly deposited on the bare gold.

To tune the selectivity of SAM deposition and thus the etch contrast, MUD was deposited on a PTMP-patterned substrate (Figure 7b). Because of its hydroxyl end-group functionality, MUD is thought to interact differently with the hydrophilic PTMP monolayer than the methyl-terminated ODT. In this case, the etch contrast was excellent. In the regions in which PTMP was patterned and outside the regions of the grown edges, a similarly low etch protection was observed. The grown MUD SAMs, in contrast, provided a high etch resistance. This resulted in well-defined isolated structures, which closely followed the edges of the PTMP pattern, regardless of its shape (e.g., in Figure 7b, the number 1 is clearly outlined). The smallest feature width measured thus far was 570 $\pm$ 30 nm.

Discussion

Ink migration across a preformed (template) monolayer requires a matching of the two inks to create a net driving force for spreading. Thermodynamically, a gradient in chemical potential is the driving force for change. In the here proposed configuration, the gradient in chemical potential results from a gradient in surface concentration, but also from differences in the relevant interfacial free energies, which may counteract the effect of the concentration gradient. It follows that, not only is the nature of the inks relevant in the design of such a scheme, but the order of their application is as well. No evidence was found for MHDA migration across a preformed ODT monolayer, despite the relatively large extent of MHDA spreading across bare gold. This is contrary to the inverse case, in which ODT was found to form a thin rim around the preformed MHDA pattern, although the extent of ODT self-spreading was significantly smaller.

The curvature of the MHDA domain edge in the region where the MHDA, ODT, and gold domains meet is an indication of the

(38) Delamarche, E.; Geissler, M.; Wolf, H.; Michel, B. *J. Am. Chem. Soc.* **2002**, *124*, 3834−3835.

importance of the interfacial energies. Because the observed structures are away from thermodynamic equilibrium, however, it was not possible to quantitatively analyze the relevant interfacial energies. From the literature values of the surface free energies of ODT ($\gamma_{ODT} = 22 \times 10^{-3}$ J/m^2) and MHDA ($\gamma_{MHDA} = 50 \times 10^{-3}$ J/m^2) it may, nevertheless, be expected that ODT will spread more easy across MHDA monolayers than vice versa.[39] This is consistent with the above observations.

Growth of a SAM guided by the template monolayer pattern may also take place without direct contact with the stamp during the second printing step. The selective growth of one monolayer from the edges of another, in the absence of direct contact, will in the following be denoted *"heteronucleation"*. Conversely, the term *"homonucleation"* is used for the case of growth without direct contact when both the growing edge and the template pattern are composed of the same ink. Homonucleation reflects the part of the spreading process in μCP in which the vapor-phase contribution is isolated from other contributions. From the observation that the rate of ODT homonucleation is consistently smaller than that of ODT self-spreading (Figure 6b), it can be inferred that, in the μCP of ODT, ink deposition from the vapor phase contributes only in a small amount to the total extent of spreading. From the observation of pattern size increase and the exclusion of a major contribution from the vapor phase, it follows that a large part of the ink transport takes place across the surface of the monolayer-covered domains. This contradicts earlier reports of autophobic pinning (i.e., the dewetting of a SAM precursor on an already formed SAM, thus self-limiting the amount of spreading) in alkanethiol SAM formation.[40−42]

Whereas spreading across a preformed monolayer is in accordance with the moving boundary model for monolayer spreading as discussed for DPN,[29,33] the observation of both homo- and heteronucleation calls for a refinement of this model for μCP. Spreading in μCP takes place in the confinement of a micro-cavity enclosed by stamp material and substrate. If volatile inks are used, an appreciable ink vapor pressure is therefore reached quickly. Mass transport from a vapor phase in μCP has already been recognized as giving rise to a background of randomly adsorbed molecules in the noncontacted areas.[4] Adsorption from a gas phase can be described by a Langmuir isotherm up to 80−90% coverage.[43] For higher coverages, deviations occur. This indicates that the presence of a molecule at an adsorption site influences the adsorption probability at neighboring sites. The kinetics of adsorption at defect sites in a dense monolayer are therefore different from the kinetics of adsorption on bare gold. The edge of a dense monolayer domain effectively constitutes such a defect. Several mechanisms may account for this cooperative adsorption and the observed preferential growth from an alkanethiol vapor onto the edges of an initially present SAM pattern (Figure 8). Molecules that are incorporated in the growing edge arrive there either directly from the gas phase (pathway iii), or after having migrated either across the bare substrate surface (pathway ii) or across the monolayer covered surface (pathway i). The cross-section for adsorption is, by far, the smallest for pathway iii. The contribution of which is therefore expected to be small.

Molecules that are deposited on the bare gold (pathway ii in Figure 8) are mobile initially, as is evident from the evolution

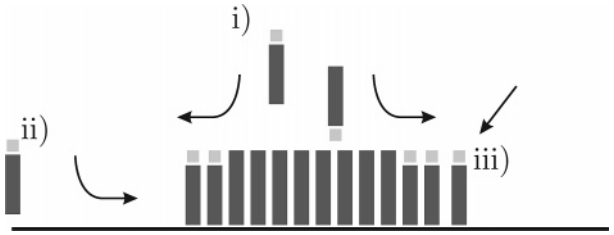

Figure 8. Schematic representation of pathways that can contribute to lateral growth of a template monolayer. Ink may deposit on the template, across which it migrates until it nucleates at the template's edge (i). Similarly, ink may deposit on the bare gold where it remains mobile until it is incorporated in a dense monolayer (ii). Alternatively, ink that arrives directly at a site neighboring the growing edge from the gas phase may have an increased sticking probability because of interactions with the existing monolayer (iii).

of distinct ordered phases as a function of surface coverage.[27,44,45] Specifically for higher surface coverage, however, immobile dense phase domains may nucleate. Good contrast between edge growth and random deposition is, therefore, only to be expected when the surface coverage on the bare gold domains remains sufficiently low throughout the deposition process, so as to maintain ink mobility. Migration toward, and incorporation into the growing edge, therefore, should be fast with respect to the net rate of adsorption on the bare gold domains. Ink adsorbed on the monolayer domains (pathway i in Figure 8), on the other hand, does not adversely affect the contrast; therefore, no such constraint is imposed on the ratio between the rate of adsorption on monolayer domains and the rate of migration across them. The basic assumption of the moving boundary transport model is that ink molecules on top of a monolayer remain highly mobile. An increased net adsorption on the monolayer-covered regions, therefore, directly translates to a higher rate of edge growth. The selectivity of edge growth is thus governed by the contrast in the net adsorption rates for the monolayer-covered and bare gold domains.

The above argumentation is corroborated by the results obtained for MUD deposition on MHDA or ODT template patterns. It shows that the rate of edge growth can be tuned by choosing a suitable composition of the template patterns in relation to the adsorbing ink, thereby adjusting the contrast in net adsorption for the bare gold and the prepatterned regions. In these studies, MUD was selected as a potentially reactive ink that enables the formation of dense monolayers but also readily deposits from a vapor.[46] This could not be achieved with MHDA, for which no detectable adsorption could be observed in the noncontact areas, even after printing of up to 4 h.[28] Interestingly, MUD growth on ODT was consistently found to be larger, for similar feature sizes of the second printing step (vapor exposure), than MUD growth on MHDA. If the adsorption probability is the rate-limiting step, this indicates that the interactions of the apolar alkyl chains contribute more to the adsorption probability than do the potential polar headgroup (−COOH/−OH) interactions. Conversely, if the mobility across the prepatterned SAM and subsequent incorporation at the growing edge is the rate-limiting step, this indicates that MUD molecules are more mobile across ODT SAMs than across MHDA SAMs. In view of the potential for (−COOH/−OH) interactions for MUD growth on MHDA, the latter appears to be the most likely explanation for the observed difference in growth rate. These observations indicate a significant contribution of vapor-transport in μCP in addition to liquid−

(39) Chaudhury, M. K.; Whitesides, G. M. *Science* **1992**, *255*, 1230−1232.
(40) Biebuyck, H. A.; Whitesides, G. M. *Langmuir* **1994**, *10*, 4581−4587.
(41) Xia, Y.; Whitesides, G. M. *J. Am. Chem. Soc.* **1995**, *117*, 3274−3275.
(42) Tien, J.; Xia, Y.; Whitesides, G. M. In *Thin Films*; Ulman, A., Ed.; Academic Press: New York, 1998; Vol. 24, pp 227−254.
(43) Dannenberger, O.; Buck, M.; Grunze, M. *J. Phys. Chem. B* **1999**, *103*, 2202−2213.
(44) Poirier, G. E.; Fitts, W. P.; White, J. M. *Langmuir* **2001**, *17*, 1176−1183.
(45) Fitts, W. P.; White, J. M.; Poirier, G. E. *Langmuir* **2002**, *18*, 2096−2102.
(46) Zamborini, F. P.; Crooks, R. M. *Langmuir* **1998**, *14*, 3279−3286.

film-assisted transport such as the liquid meniscus transport, which is thought to govern the spreading in DPN.[22]

If the composition of the template pattern is fixed (e.g., because of a desirable functionality), the second deposited ink must be chosen accordingly. PTMP, which is relatively hydrophilic, interacts more strongly with the hydroxyl-terminated MUD than with the methyl-terminated ODT.[38] MUD, for this reason, accumulates more readily on PTMP. The observed more selective edge growth of MUD on a PTMP SAM is, therefore, in accordance with the previous analysis. It follows that growth of MUD edge features on preformed PTMP SAMs is highly suitable for the creation of submicrometer-sized gold features via μCP with micrometer-sized stamp structures and subsequent chemical etching.

Conclusions

The formation of alkanethiol edge structures on two-dimensional scaffolds was investigated. It was shown that prepatterned monolayers can be used as scaffolds for the directed self-assembly of heterostructures. For the case in which a preformed monolayer was contacted with an ink-loaded stamp during a second printing step, monolayer spreading in μCP could be described by a "moving boundary" transport model, in which molecules cross a preformed monolayer before adhering to the growing edge. Autophobic pinning of ODT was not observed. In addition, a gas-phase contribution to lateral growth was identified. The mechanism for lateral growth of ODT on prepatterned MHDA is most probably governed by an indirect adsorption process, that is, the adsorption of ink on the preexisting monolayer followed by migration to the growing edge. The selectivity of edge growth over random adsorption can be tuned by choosing a suitable template/donor ink system, taking into account the relevant interfacial energies. MUD has been identified as a useful ink for the selective growth of edge features from a vapor phase on template patterns of ODT, MHDA, and PTMP. Its favorable attributes include its high vapor pressure, its functional end group, and the observed contrast in etch resistance between dense and diluted monolayers.

The contrast in chemical functionality between the monolayer and bare gold domains may be exploited in several ways. The contrast in hydrophobicity may, for example, be utilized for the selective physisorption of colloids, proteins, or cells, and the contrast in reactivity may, for example, be exploited for subsequent selective amplification of one of the monolayers. In this report, it has been shown that, as an example of an application, the contrast in the properties of the template monolayer, the selectively grown edges, and the substrate can be used for the selective etching of gold, thereby transferring the edge pattern into the substrate.

Control over the position, orientation, and surface chemistry of the template offers a great potential for downscaling and a clear advantage over conventional methods for nanowire growth. Specifically the control over the surface chemistry (or rather "edge chemistry") allows for the design of schemes for self-limiting lateral growth. This may allow for the growth of self-assembled one-dimensional molecular wires in a manner analogous to two-dimensional SAM growth.

Acknowledgment. This work is part of the research program of the Stichting voor Fundamenteel Onderzoek der Materie (FOM, financially supported by the Nederlandse Organisatie voor Wetenschappelijk Onderzoek (NWO) and Philips Research). R.S. gratefully acknowledges the hospitality of the group "Bio-Molecular Engineering", Philips Research, The Netherlands. The authors furthermore thank Michel M. J. Decré (Philips Research) for carefully reviewing this manuscript.

LA061787V